Defense Technical Information Center Compilation Part Notice

ADP011030

TITLE: Generalized Ellipsometry Using a Rotating Sample

DISTRIBUTION: Approved for public release, distribution unlimited

This paper is part of the following report:

TITLE: Materials Research Society Symposium Proceedings Volume 635. Anisotropic Nanoparticles - Synthesis, Characterization and Applications

To order the complete compilation report, use: ADA395000

The following component part numbers comprise the compilation report:
ADP011010 thru ADP011040

Mat. Res. Soc. Symp. Proc. Vol. 635 © 2001 Materials Research Society

Generalized Ellipsometry Using a Rotating Sample

Weiliang Xu*, Lowell T. Wood, and Terry D. Golding**
Department of Physics, University of Houston, Houston, Texas 77204-5506, U.S.A.

ABSTRACT

We propose a generalized ellipsometric technique using a rotating sample. The ellipsometer consists of a polarizer, a rotatable sample holder, an analyzer, and a detector. Fourier coefficients are measured and used to extract the system's dielectric tensors and film thicknesses. The main advantage of the technique is that all parts of the ellipsometer are fixed except the sample, whose azimuth angle can be modulated. We show calculated responses to isotropic and anisotropic materials as well as superlattices. Potential applications for characterizations of anisotropic nanostructures are discussed.

I. INTRODUCTION

In a conventional rotating element ellipsometer, only one variable, i.e., the azimuth angle of the rotating element, is changed in the characterization of an isotropic material. In current generalized ellipsometers for characterizing anisotropic systems, however, either additional variables [1], e.g., the angle of incidence and the azimuth angles of the polarizer (or analyzer) and of the sample, are changed, or components not commonly found in a conventional rotating element ellipsometer are needed [2,3]. Even in the simplest case of uniaxial materials, two variables, i.e., the azimuth angles of the polarizer and analyzer, are required if sets of Ψ and Δ are measured to determine the dielectric tensors of the materials [4]. Optimization of ellipsometric setups with fewer variables involved in measurements is highly desirable in situations where measurements are remotely controlled, since the reliability of the controls and the accuracy of the measured data are improved. One such situation is the characterization of samples grown in space. In this paper we present a theoretical development and show that changing only the sample's azimuth angle is sufficient to determine dielectric tensors and film thicknesses of arbitrarily anisotropic systems. Instead of Ψ and Δ, the intensity dependence on the sample's azimuth angle is measured. Two approaches for analysis are proposed to determine the dielectric tensors and film thicknesses from the measured intensities. Popular conventional ellipsometer setups, e.g., polarizer-compensator-sample-analyzer (PCSA) or polarizer-sample-analyzer (PSA), can use this approach to characterize anisotropic systems by keeping all components fixed except the sample.

II. THEORY

In this section, we study the dependence of intensity on α_S, the sample's azimuth angle, to permit extraction of the dielectric tensors and film thicknesses. For an n-layer anisotropic

---

* Present address: DigiBot Inc., 4006 Beltline, Suite 234, Addison, TX 75001, wxu@digibotinc.com.
** Present address: Department of Physics, University of North Texas, TX 76203, golding@unt.edu

system, following the same procedure and coordinates setup as in Refs. [4,5], the Jones matrix (r) for reflection ellipsometry is

$$r_{pp} = \left(T_{31}T_{22} - T_{32}T_{21}\right)/\left(T_{11}T_{22} - T_{12}T_{21}\right), \tag{1}$$

$$r_{ps} = \left(T_{32}T_{11} - T_{31}T_{12}\right)/\left(T_{11}T_{22} - T_{12}T_{21}\right), \tag{2}$$

$$r_{sp} = \left(T_{41}T_{22} - T_{42}T_{21}\right)/\left(T_{11}T_{22} - T_{12}T_{21}\right), \tag{3}$$

$$r_{ss} = \left(T_{42}T_{11} - T_{41}T_{12}\right)/\left(T_{11}T_{22} - T_{12}T_{21}\right), \tag{4}$$

where (T) is the transfer matrix of the system. The formula for calculating (T) can be found elsewhere [6]. These expressions establish the relationships between the Jones matrix and the system's dielectric tensors and film thicknesses. For layer i, if we use the diagonal tensor $(\varepsilon_l)_i$, l=1, 2, 3, to represent the dielectric tensor with respect to its principal axes, Θ_i=(θ_{ri}, ϕ_{ri}, φ_{ri}, θ_{ii}, ϕ_{ii}, φ_{ii}) for the Euler angles of the frame of principal axes with respect to the laboratory frame for the real and imaginary parts of the dielectric tensor, and d_i for the thickness, (T) is completely determined by $(\varepsilon_l)_i$, Θ_i, and d_i, (i=1,…n).

If the PSA setup is used, the intensity after the analyzer is

$$I_d = I_p \left| \left(r_{pp}\cos\alpha_{\mathrm{P}} + r_{sp}\sin\alpha_{\mathrm{P}}\right)\cos\alpha_{\mathrm{A}} + \left(r_{ps}\cos\alpha_{\mathrm{P}} + r_{ss}\sin\alpha_{\mathrm{P}}\right)\sin\alpha_{\mathrm{A}} \right|^2, \tag{5}$$

where I_d is the intensity reaching the detector, I_p is a constant, and α_{P} and α_{A} are the azimuth angles of the polarizer and analyzer, respectively.

If α_{P} and α_{A} are fixed, changing α_{S}, i.e., rotating the sample, leads to the change of $\phi_i = (\phi_{ri}, \phi_{ii})$. Recall that the transfer matrix (T) depends on ϕ_i. Therefore, the Jones matrix changes with α_{S} and so does the intensity. However, the dielectric tensors on the principal axis frame and the Euler angles θ_i and φ_i remain the same. Substitution of Eqs. (1) – (4) into Eq. (5) gives I_d a function h of the dielectric tensors and film thicknesses. That is,

$$I_d(\alpha_{\mathrm{S}}) = I_p h((\underline{\varepsilon_l})_i, \underline{\theta}_{ri}, \underline{\phi}_{ri0} + \alpha_{\mathrm{S}}, \underline{\varphi}_{ri}, \underline{\theta}_{ii}, \underline{\phi}_{ii0} + \alpha_{\mathrm{S}}, \underline{\varphi}_{ii}, \underline{d}_i), \tag{6}$$

where the underlined parameters do not change when the sample rotates, and ϕ_{ri0} and ϕ_{ii0} are the initial angles for ϕ_{ri} and ϕ_{ii}.

From Eq. (6), if the total number of $(\varepsilon_l)_i$, θ_{ri}, ϕ_{ri0}, φ_{ri}, θ_{ii}, ϕ_{ii0}, φ_{ii}, and d_i is k, and I_p is taken as unknown, they can, in principle, be determined by $k+1$ independent equations between I_d and I_p, $(\varepsilon_l)_i$, θ_{ri}, ϕ_{ri0}, φ_{ri}, θ_{ii}, ϕ_{ii0}, φ_{ii}, and d_i. In the rest of this section, we discuss two approaches of changing α_{S} to establish m ($m \geq k+1$) equations between I_d and I_p, $(\varepsilon_l)_i$, θ_{ri}, ϕ_{ri0}, φ_{ri}, θ_{ii}, ϕ_{ii0}, φ_{ii}, and d_i.

Approach one:

The intuitive way to establish m ($m \geq k+1$) equations between I_d and I_p, $(\varepsilon_l)_i$, θ_{ri}, ϕ_{ri0}, φ_{ri}, θ_{ii}, ϕ_{ii0}, φ_{ii}, and d_i is to set α_{S} to m different settings. If the intensities $I_d(\alpha_{\mathrm{S}1})$, $I_d(\alpha_{\mathrm{S}2})$, …, $I_d(\alpha_{\mathrm{S}m})$ have been measured, m equations are set up. They are

$$I_p h((\underline{\varepsilon_l})_i, \underline{\theta}_{ri}, \underline{\phi}_{ri0} + \alpha_{\mathrm{S}1}, \underline{\varphi}_{ri}, \underline{\theta}_{ii}, \underline{\phi}_{ii0} + \alpha_{\mathrm{S}1}, \underline{\varphi}_{ii}, \underline{d}_i) = I_d(\alpha_{\mathrm{S}1}), \tag{7}$$

$$I_p h((\underline{\varepsilon}_l)_i, \underline{\theta}_{ri}, \underline{\phi}_{ri0}+\alpha_{S2}, \underline{\varphi}_{ri}, \underline{\theta}_{ii}, \underline{\phi}_{ii0}+\alpha_{S2}, \underline{\varphi}_{ii}, \underline{d}_i)= I_d(\alpha_{S2}), \tag{8}$$

.....

$$I_p h((\underline{\varepsilon}_l)_i, \underline{\theta}_{ri}, \underline{\phi}_{ri0}+\alpha_{Sm}, \underline{\varphi}_{ri}, \underline{\theta}_{ii}, \underline{\phi}_{ii0}+\alpha_{Sm}, \underline{\varphi}_{ii}, \underline{d}_i)= I_d(\alpha_{Sm}). \tag{9}$$

To solve these equations for I_p, $(\varepsilon_l)_i$, θ_{ri}, ϕ_{ri0}, φ_{ri}, θ_{ii}, ϕ_{ii0}, φ_{ii}, and d_i, a test function is introduced:

$$Err=\sum_{j=1}^{m}\left[I_p h\left((\varepsilon_l)_i,\theta_{ri},\phi_{ri0}+\alpha_{Sj},\varphi_{ri},\theta_{ii},\phi_{ii0}+\alpha_{Sj},\varphi_{ii},d_i\right)-I_d(\alpha_{Sj})\right]^2\Big/\sigma_j^2, \tag{10}$$

where σ_j is the standard deviation for $I_d(\alpha_{Sj})$. Ideally, if there are no errors in the measurements of I_d, Eq. (10) reduces to Eqs. (7) – (9) if Err is minimized to zero. In practice, errors exist in I_d, but Err can be reduced to a minimum value. The I_p, $(\varepsilon_l)_i$, θ_{ri}, ϕ_{ri0}, φ_{ri}, θ_{ii}, ϕ_{ii0}, φ_{ii}, and d_i that minimize Err can be taken as the true values. We outline the algorithm for the minimization and discuss the error distribution in determining $(\varepsilon_l)_i$, θ_{ri}, ϕ_{ri0}, φ_{ri}, θ_{ii}, ϕ_{ii0}, φ_{ii}, and d_i.

For clarity of notation, we use x_l, $l = 1, 2, \ldots, k, k+1$ to represent the k variables of $(\varepsilon_l)_i$, θ_{ri}, ϕ_{ri0}, φ_{ri}, θ_{ii}, ϕ_{ii0}, φ_{ii}, d_i, and I_p, and define a vector $X^T=(x_1, x_2, \ldots, x_{k+1})$, where the superscript T denotes the transpose of the column vector X. When Err reaches its minimum,

$$\left(\partial Err/\partial x_l\right)_t = 0,\ l = 1, 2, \ldots, k+1, \tag{11}$$

where the subscript t means that x_l, i.e., $(\varepsilon_l)_i$, θ_{ri}, ϕ_{ri0}, φ_{ri}, θ_{ii}, ϕ_{ii0}, φ_{ii}, and d_i, assume the true values of the dielectric tensors and film thicknesses. Using matrix notation, Eq. (11) can be simply denoted as

$$\nabla Err = 2A^T \mathrm{H} = 0, \tag{12}$$

where

$$\mathrm{H}=(h_1, h_2, \ldots, h_m)^T, \tag{13}$$

$$h_j = I_p h\left((\varepsilon_l)_i,\theta_{ri},\phi_{ri0}+\alpha_{Sj},\varphi_{ri},\theta_{ii},\phi_{ii0}+\alpha_{Sj},\varphi_{ii},d_i\right)-I_d(\alpha_{Sj}),\ j=1,2,\ldots,m, \tag{14}$$

$$A_{jl}=\left(\partial h_j/\partial x_l\right)_t\Big/\sigma_j^2,\ j=1,2,\ldots,m;\ l=1,2,\ldots,k+1. \tag{15}$$

Near the minimum of Err, H can be linearized as $\mathrm{H}=\mathrm{H}_t + A\Delta X$, and substituting it into Eq. (12) obtains

$$\Delta X = -\left(A^T A\right)^{-1} A^T \mathrm{H}_t = -\mathrm{M}A^T\mathrm{H}_t. \tag{16}$$

Eq. (16) gives an expression for changing X recursively to minimize Err. The standard deviation of x_l, $l=1, 2, \ldots, k, k+1$, determined with the above algorithm, is [8]

$$\sigma_{x_l}^2 = \mathrm{M}_{ll}. \tag{17}$$

Approach two:

Instead of setting a sample to different discrete angles, the sample can be rotated at a constant frequency ω. That is, $\alpha_S = \omega t$. In this case, Eq. (6) can be expressed as

$$I_d(\omega t) = I_p \sum_l \left(a_l \cos l\omega t + b_l \sin l\omega t \right), \tag{18}$$

where a_l and b_l are the Fourier coefficients.

If $m=2j+1$, $m \geq k+1$, Fourier coefficients a_0, a_1, b_1, ..., a_j, b_j, are measured, m equations of $(\varepsilon_l)_i$, θ_{ri}, ϕ_{ri0}, φ_{ri}, θ_{ii}, ϕ_{ii0}, φ_{ii}, and d_i can be established. They are

$$\frac{1}{tI_p}\int_0^t h\left((\varepsilon_l)_i, \theta_{ri}, \phi_{ri0}+\alpha, \varphi_{ri}, \theta_{ii}, \phi_{ii0}+\alpha, \varphi_{ii}, d_i\right) d\alpha = a_0, \tag{19}$$

....

$$\frac{2}{tI_p}\int_0^t h\left((\varepsilon_l)_i, \theta_{ri}, \phi_{ri0}+\alpha, \varphi_{ri}, \theta_{ii}, \phi_{ii0}+\alpha, \varphi_{ii}, d_i\right) \cos j\alpha d\alpha = a_j, \tag{20}$$

$$\frac{2}{tI_p}\int_0^t h\left((\varepsilon_l)_i, \theta_{ri}, \phi_{ri0}+\alpha, \varphi_{ri}, \theta_{ii}, \phi_{ii0}+\alpha, \varphi_{ii}, d_i\right) \sin j\alpha d\alpha = b_j, \tag{21}$$

where $t \leq 2\pi$ is the smallest period of function h.

To solve Eqs. (19) – (21), a test function

$$Err = \sum_{l=0}^{j} \left(\frac{2\int_0^t h \cos l\alpha d\alpha}{(1+\delta_{l0}) tI_p} - a_l \right)^2 \Big/ \sigma_l^2 + \sum_{l=1}^{j} \left(\frac{2\int_0^t h \sin l\alpha d\alpha}{tI_p} - b_l \right)^2 \Big/ \sigma_l^2, \tag{22}$$

is introduced, where σ_l are the standard deviations for the Fourier coefficients.

The algorithm outlined in Approach one can be employed to solve Eqs. (19) – (21), if the intensities are replaced by the Fourier coefficients and the function h replaced by the Fourier integrals. Eq. (17) can also be used to estimate the error distributions of $(\varepsilon_l)_i$, θ_{ri}, ϕ_{ri0}, φ_{ri}, θ_{ii}, ϕ_{ii0}, φ_{ii}, and d_i.

If j is large, direct measurements of the Fourier coefficients may be inconvenient. In this situation, the intensity dependence on the sample's azimuth angle can be measured. With this relation, the Fourier coefficients can be obtained numerically. It should be noted that if $t<2\pi$, all α_S selected in Approach one should not be different by t. If $t=0$, i.e., I_d is constant, only a_0 is meaningful. In this case, this method fails.

III. MODELS CALCULATION

In this section, we prescribe the dielectric tensors and film thicknesses of some common structures and conduct forward calculation for the intensity dependence on sample's azimuth angle. The purpose of the study is to show that different structures possess different relationships between intensity and sample's azimuth angle. Therefore, from a measured intensity dependence on sample's azimuth angle, a backward calculation can extract the dielectric tensors and film thicknesses by use of the two approaches described in the previous section.

In the study, we assume that the angle of incidence is 70°, and the wavelength is 600nm. All materials are transparent for simplicity. A PSA setup is used and $\alpha_P = \alpha_A = 45^\circ$. An isotropic material, two bulk anisotropic materials (uniaxial and biaxial) are studied. The isotropic and uniaxial materials are also used as the substrates of a superlattice structure, which is 20 periods of a two-layer structure on a substrate. They can be denoted as *ABAB...ABC*, where *A* and *B* are biaxial films, and *C* is substrate. The properties of these materials are listed in Table I. Relations between intensities and sample's azimuth are shown in Figure 1. Parts of the Fourier coefficients are listed in Tables II.

Figure 1 shows that the intensity relationships are different for different structures. Table II shows that except for isotropic materials, all other structures contain more non-zero Fourier coefficients than unknowns. Therefore, Eq. (22) can be used. For isotropic materials, Figure 1 shows that the intensity is a constant. As stated in the above section, this method fails in this case. One interesting observation is that in Figure 1, two superlattices show difference mainly near extremum positions. However, Table II shows that all Fourier coefficients have distinct difference. This fact implies that if Approach one is used, α_S has to be set near extremum positions so that the difference can be detected. However, Approach two does not have this limitation.

Table I. Refractive indices of different materials along their principal axes, Euler angles of the principal axes relative to the laboratory frame, thicknesses of the materials and number of parameters that can be determined.

	n_1	n_2	n_3	θ	ϕ_0	φ	d (nm)	k
Isotropic	1.8	1.8	1.8	any	any	any	∞	1
Uniaxial	1.8	1.8	2.0	20	60	any	∞	4
Biaxial	1.8	2.0	2.2	20	60	10	∞	6
Layer *A*	1.6	1.7	1.8	45	35	10	300	7
Layer *B*	1.5	1.6	1.7	30	20	30	600	7

Table II. Fourier coefficients a_l and b_l for the intensity $I_d(\omega t) = I_p \sum (a_l \cos l\omega t + b_l \sin l\omega t)$.
Lattice 1 (resp. 2) is a 40-layer periodic superlattice on an isotropic (resp. uniaxial) substrate.

	a_0	a_1, b_1 (10^{-3})	a_2, b_2 (10^{-3})	a_3, b_3 (10^{-5})	a_4, b_4 (10^{-6})	a_5, b_5 (10^{-6})	a_6, b_6 (10^{-6})	a_7, b_7 (10^{-6})	a_8, b_8 (10^{-6})
Isotropic	.2665	0,0	0,0	0,0	0,0	0,0	0,0	0,0	0,0
Uniaxial	.2581	6.235 -10.80	2.045 3.542	3.500 0	-2.000 0	0,0	0,0	0,0	0,0
Biaxial	.2492	3.867 -4.329	17.89 16.44	9.900 -1.100	11.00 128.0	-1.000 -1.000	2.000 -2.000	0,0	0,0
Lattice 1	.2913	21.40 5.696	-22.87 16.50	914.0 4113	10290 5194	3050 10450	12930 -619.0	-35210 -29820	-16710 -5554
Lattice 2	.2936	23.38 12.77	-26.12 12.67	852.0 3941	11770 4137	3333 11640	10610 312	-34730 -29630	-17730 -4792

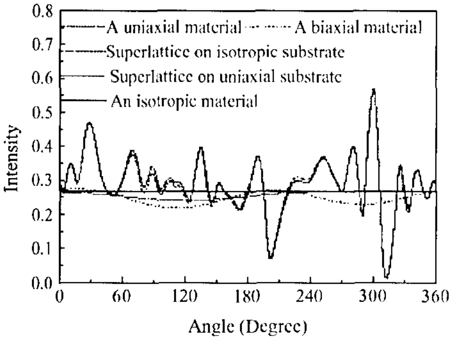

Figure 1. Intensity dependence on sample's azimuth angle for (1) an isotropic material, (2) a uniaxial material, (3) a biaxial material, (4) a 40-layer periodic superlattice on the isotropic substrate, and (5) a 40-layer periodic superlattice on the uniaxial substrate.

IV. SUMARY

In this paper, we present a theoretical development to optimize a generalized ellipsometer so that only the sample's azimuth angle needs to be changed in the determination of the dielectric tensors and film thicknesses of a arbitrarily anisotropic systems. Five models are calculated as examples.

ACKNOWLEDGEMENTS

This work was supported in part by the Advanced Technology Program and Advanced Research Program of the Texas Higher Education Coordinating Board, the Texas Center for Superconductivity at the University of Houston, and the Robert. A. Welch Foundation.

REFERENCES

[1] D. W. Thompson, M. J. DeVries, T. E. Tiwald, and J. A. Woollam, *Thin Solid Films* **313-314**, 341 (1998).
[2] G. E. Jellison and L. A. Boatner, *Phys. Rev. B* **58**, 3586 (1998).
[3] R. W. Collins and J. Koh, *J. Opt. Soc. Am. A* **16**,1997 (1999).
[4] W. Xu, L. T. Wood, and T. D. Golding, *Thin Solid Films* (To be published).
[5] W. Xu, L. T. Wood, and T. D. Golding, *J.Opt. Soc. Am A* (Submitted for publication).
[6] W. Xu, L. T. Wood, and T. D. Golding, *Phys. Rev. B.* **61**, 1740 (2000).
[7] P. Yeh, *J. Opt. Soc. Am.* **69**, 742 (1979).
[8] P. R. Bevington, Data Reduction and Error Analysis for the Physical Sciences, Mc-Graw-Hill Book Company, New York. p. 242.